

## Effect of synthesis method on the structural, conductive and sensor properties of NiO–In<sub>2</sub>O<sub>3</sub> nanocomposites

Mariya I. Ikim<sup>1,a</sup>, Vladimir F. Gromov<sup>1,b</sup>, Genrikh N. Gerasimov<sup>1,c</sup>, Valentin G. Bekeshev<sup>1,d</sup>, Leonid I. Trakhtenberg<sup>1,2,3,c</sup>

<sup>1</sup>N. N. Semenov Federal Research Center for Chemical Physics RAS, Moscow, Russia

<sup>2</sup>Chemical Faculty, Lomonosov Moscow State University, Moscow, Russia

<sup>3</sup>Moscow Institute of Physics and Technology(State University), Moscow, Russia

<sup>a</sup>ikimmary1104@gmail.com, <sup>b</sup>vfgromov@mail.ru, <sup>c</sup>gerasimovgen@mail.ru, <sup>d</sup>bvg495@yandex.ru,

<sup>e</sup>litrah@gmail.com

Corresponding author: Mariya I. Ikim, ikimmary1104@gmail.com

PACS 73.63.-b

**ABSTRACT** The structural, conductive and sensor properties of NiO–In<sub>2</sub>O<sub>3</sub> composites synthesized by hydrothermal and impregnation methods are investigated and compared. The mixed oxide considered consists of nanoparticles with electronic (In<sub>2</sub>O<sub>3</sub>) and hole (NiO) conduction bands. The lattice parameters of indium oxide decrease with the introduction of NiO into composites synthesized by the hydrothermal method. The addition of 3 % NiO to the hydrothermal composite also increases its specific surface area. The specific surface area and In<sub>2</sub>O<sub>3</sub> lattice parameters in the impregnated samples are essentially independent of the NiO content. The conductivity of impregnated composites is an order of magnitude lower than that of hydrothermal composites. An increase in NiO content leads to a significant enhancement of the sensor response to H<sub>2</sub> and CO. In addition, there is a decrease in the optimal operating temperature of hydrothermal and impregnated samples by 60 and 20 °C, respectively.

**KEYWORDS** composite, hydrothermal method, impregnation, indium oxide, conductivity, sensor response, hydrogen, carbon monoxide

**ACKNOWLEDGEMENTS** The work was supported by the Russian Science Foundation (grant No. 22-19-00037).

**FOR CITATION** Ikim M.I., Gromov V.F., Gerasimov G.N., Bekeshev V.G., Trakhtenberg L.I. Effect of synthesis method on the structural, conductive and sensor properties of NiO–In<sub>2</sub>O<sub>3</sub> nanocomposites. *Nanosystems: Phys. Chem. Math.*, 2024, **15** (6), 867–878.

### 1. Introduction

The presence in the atmosphere of various gases that can have harmful effects on human health has led to the development of research aimed at effective detection of these compounds. A considerable attention has been paid to the detection of reducing compounds such as H<sub>2</sub>, CO, CH<sub>4</sub>, NH<sub>3</sub> and others. One of the most effective detection methods is the use of metal oxide compounds whose conductivity changes in the presence of the above-mentioned reducing gases.

Previous studies have shown that mixtures of n-type metal oxides with different conductivity and catalytic activity can be used as sensors for detection of reducing and oxidizing gases (see, for example, [1–4]). However, despite the enough high sensitivity of the oxides considered in these studies, such as SnO<sub>2</sub>, In<sub>2</sub>O<sub>3</sub>, CeO<sub>2</sub>, ZnO, their sensor effect is fully observed only at sufficiently high temperatures, usually above 400 °C. In addition, metal oxide-based composites with an electronic type of conductivity are characterized by relatively low selectivity.

The gas sensitivity of p-type metal oxides is generally much lower than that of n-type metal oxides [5], however, their efficiency and selectivity are manifested at significantly lower temperatures (from room temperature to 150 – 200 °C). The use of mixtures consisting of n- and p-type metal oxides for detection can lead to more efficient composites. In this regard, the creation of p-n or n-p heterojunctions is one of the most important methods for obtaining metal oxide sensor materials. The formation of p-n heterostructures, as well as the introduction of p-type metal oxide into an n-type semiconductor produces an increase in the specific surface area of the composites, an increase in the number of active centers and more intensive generation of adsorbed oxygen due to the formation of an extended electron-depleted layer in the p-n junction [6–10].

The Fermi level for n-type metal oxides is higher than for p-type compounds. Therefore, in a mixture of such oxides, electrons with higher energy will transfer from the n-type metal oxide across the interface to unoccupied states with lower energy, which will lead to an equalization of the Fermi energy of both components. The potential barrier that must be

overcome in the process of such electron transfers increases or decreases significantly in the presence of oxidizing and reducing gases, respectively, while ensuring the occurrence of a sensory effect (see, for example, paper [11]).

Indeed, the addition of even small amounts of p-type semiconductor  $\text{Co}_3\text{O}_4$  to  $\text{In}_2\text{O}_3$  having electronic conductivity leads to a significant increase in the sensor response to hydrogen [12]. In addition, when detecting  $\text{H}_2\text{S}$ , the  $\text{ZnO-CuO}$  nanofiber has a higher sensor activity compared to the  $\text{ZnO}$  nanofiber [13]. The sensitivity to  $\text{H}_2\text{S}$  of  $\text{CuO-doped SnO}_2$  nanofibers increases relative to the undoped  $\text{SnO}_2$ -based layer [14].

One of the components of sensor materials is nickel oxide, which has strong oxidizing properties, excellent catalytic activity and good electrical conductivity [15, 16]. The addition of metal oxides such as  $\text{Fe}_2\text{O}_3$ ,  $\text{MoO}_3$ ,  $\text{ZnO}$ ,  $\text{WO}_3$ ,  $\text{TiO}_2$  to  $\text{NiO}$ , which is a p-type semiconductor, leads to a significant increase in sensitivity to acetone [6–10]. The response to 100 ppm acetone of  $\alpha\text{-Fe}_2\text{O}_3/\text{NiO}$  heterostructures increases by almost 7 folds over pure  $\text{NiO}$  [10]. The response of the  $\alpha\text{-MoO}_3\text{-NiO}$  composite with a core/shell structure is 6.6 times higher than that of pure  $\text{NiO}$  [6]. Hollow  $\text{NiO-SnO}_2$  particles have a much higher response to triethylamine than the original hollow spheres of  $\text{SnO}_2$  [17]. The n-p heterojunction occurring in the  $\text{SnO}_2/\text{NiO}$  system provides ultra-high sensitivity and selectivity of this material to  $\text{H}_2\text{S}$  [18].

The gas-sensitive properties of  $\text{NiO}$  nanofibers and one-dimensional heterogeneous  $\text{NiO-In}_2\text{O}_3$  nanofibers obtained by electrospinning were investigated for acetone detection [19]. It was shown that the heterogeneous nanofibers formed from  $\text{In}_2\text{O}_3$  and  $\text{NiO}$  demonstrate increased sensitivity to acetone. At the optimal operating temperature, the response of  $\text{ZnO-In}_2\text{O}_3$  nanofibers to 50 ppm of acetone was more than 10 times higher than the response of pure  $\text{NiO}$  nanofibers. The acetone detection limit for heterogeneous nanofibers reached 10 ppm, while it was 100 ppm for  $\text{NiO}$  nanofibers. The response of heterogeneous  $\text{NiO-In}_2\text{O}_3$  nanofibers to acetone exceeds the response to methanol, ethanol, triethylamine, ethyl acetate and benzene [19]. In addition, heterogeneous nanofibers have demonstrated a higher recovery rate after removal of the analyzed gas and good long-term stability. These results demonstrate that one-dimensional heterogeneous  $\text{NiO-In}_2\text{O}_3$  nanofibers have great potential for detection of low concentrations of acetone.

A significant sensor activity to ethanol of  $\text{NiO-In}_2\text{O}_3$  nanofibers obtained by electrospinning and calcination has been demonstrated [20]. The most active composite among the samples containing up to 7.5 mol. %  $\text{NiO}$  is the 5 %  $\text{NiO}$  – 95 %  $\text{In}_2\text{O}_3$  composite which has a response of 78 to 100 ppm ethanol at 300 °C. It is assumed that the improved sensor characteristics are due to the formation of p-n-transitions between  $\text{NiO}$  and  $\text{In}_2\text{O}_3$ , the ability to adsorb various forms of oxygen and an increase in the specific surface area of nanofibers when  $\text{NiO}$  is added to  $\text{In}_2\text{O}_3$ .

Here, composites consisting of  $\text{In}_2\text{O}_3$  and p-type hole conductive  $\text{NiO}$  are synthesized by the hydrothermal and impregnated methods. The effect is then investigated of the composition on the electronic state, the spatial structure of such composites, as well as their conductivity and sensor activity in the detection of  $\text{H}_2$  and  $\text{CO}$ .

## 2. The experimental part

Nickel nitrate  $\text{Ni}(\text{NO}_3)_2 \cdot 6\text{H}_2\text{O}$  (99 %) and indium nitrate  $\text{In}(\text{NO}_3)_3 \cdot 4\text{H}_2\text{O}$  (99.5 %) were used as precursors in the hydrothermal synthesis of mixed  $\text{NiO-In}_2\text{O}_3$  oxides. The required amount of nickel nitrate was added to the indium nitrate solution in distilled water or ethanol and kept in an ultrasonic bath for 1 hour at 30 °C. The solution was then placed in a Teflon-coated autoclave (volume 100 ml) and kept for 3 hours at 160 °C. The resulting suspension was separated in a centrifuge, and the powder washed with distilled water and annealed in air at 500 °C.

Commercial  $\text{In}_2\text{O}_3$  powder (AnalaR brand, 99.5 %, BDH/Merck Ltd., Lutterworth, Leicestershire, UK), as well as chemically pure  $\text{Ni}(\text{NO}_3)_2 \cdot 6\text{H}_2\text{O}$  were used to obtain  $\text{NiO-In}_2\text{O}_3$  composites by impregnation. Indium oxide nanopowder was placed in an aqueous solution of nickel nitrate with concentration of 0.015 mol/l and the resulting suspension was maintained for a long time. This treatment causes complete wetting the surface of the solid oxide by the salt solution. Moreover, salt molecules are not only adsorbed on the surface of  $\text{In}_2\text{O}_3$ , but also diffuse into its near-surface layers. To obtain impregnated samples water was removed at a temperature of about 70 – 80 °C, and the samples were subsequently heated for several hours at 500 °C. The phase composition and crystal lattice parameters of the composites synthesized by the two methods considered were determined by X-ray diffraction (XRD) using the Rigaku Smartlab GP X-ray diffractometer (CuK $\alpha$  radiation with a wavelength of 1.5406 Å). The morphology of the particles in the composites and the distribution of metal ions between the components of the composite were determined by TEM and EDX methods on a JEOL OSM-6000PLUS device equipped with an energy dispersion analysis system. The electronic structure of the composites was determined by X-ray photoelectron spectroscopy (XPS) on a Prevac EA15 spectrometer using Mg(K $\alpha$ ) (1253.6 eV) as the radiation source. The specific surface area and pore size distribution in the synthesized composites were determined by low-temperature nitrogen adsorption on the NOVA 1200e Quantachrome device (USA).

The conductivity and sensor properties were investigated in the temperature range 300 – 550 °C. The chip with the applied sensor layer was placed in a special chamber of about 1 cm<sup>3</sup> volume into which purified air or a gas mixture was supplied. The mixture consisted of purified air and  $\text{H}_2$  or  $\text{CO}$ . We used two concentrations of the analyzed gas: 0.9 or 0.1 %. The rate of gas pumping through the chamber was 200 ml/min, and the accuracy of temperature maintenance was within 1 °C. The sensor response was determined by the relation  $S = R_0/R_g$ , where  $R_0$  is the initial resistance of the sensor in air, and  $R_g$  is the minimal value of the sensor resistance after the introduction of the mixture being investigated.

The response time of the sensor  $t_{\text{resp}}$  (the time required to achieve a 90 % change in the resistance of the sensor after introducing the analyzed gas) and the recovery time of the sensor  $t_{\text{rec}}$  (the time required to reach 90 % of the initial resistance of the sensor after removal of the mixture considered) were determined by the change in the resistance of the sensor layer. The change in the sensor resistance was recorded using a Keysight digital multimeter, the signal from which was transmitted to a computer.

### 3. Results and discussion

#### 3.1. Structural characteristics of NiO–In<sub>2</sub>O<sub>3</sub> composites

X-ray analysis data show that, regardless of the synthesis method, when up to 3 wt. % NiO is added to In<sub>2</sub>O<sub>3</sub>, there are no peaks characterizing nickel or its compounds in the XRD spectra of the composite (Fig. 1). This result may be caused by the dissolution of nickel ions in the In<sub>2</sub>O<sub>3</sub> lattice, the formation of an X-ray amorphous phase, or simply the small amount of NiO in the composites. Only peaks corresponding to the cubic phase of indium oxide (c-In<sub>2</sub>O<sub>3</sub>) with a predominant orientation (222) are recorded in the spectra of impregnated and hydrothermal composites synthesized from aqueous solutions of indium and nickel nitrates (Fig. 1(1,2)). In turn, all the observed diffraction peaks in the spectra of composites synthesized from an alcohol solution of the salts belong to the rhombohedral phase of indium oxide of the corundum type (*rh*-In<sub>2</sub>O<sub>3</sub>) with a predominant orientation (104) and (110) (Fig. 1(3)).

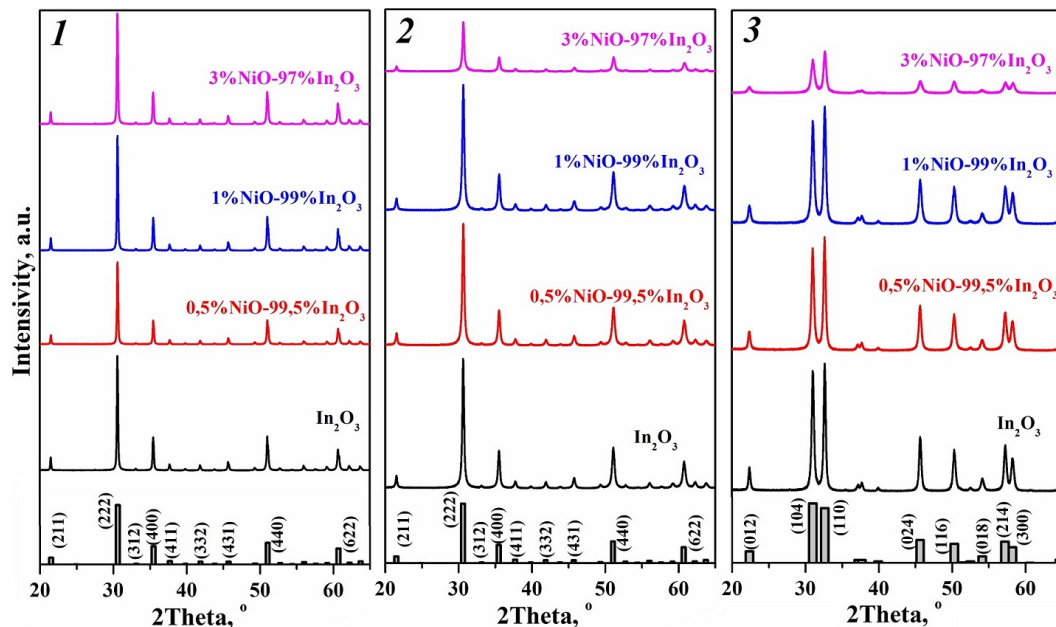


FIG. 1. XRD pattern of NiO–In<sub>2</sub>O<sub>3</sub> composites synthesized by impregnation (1) and hydrothermal method in water (2) and ethanol (3)

Increase in the nickel content in the synthesized composites results in a shift in the diffraction angles of the reflex (222) for the cubic phase and reflex (104) for the rhombohedral phase of In<sub>2</sub>O<sub>3</sub>. It can be assumed that nickel ions are embedded in the indium oxide lattice, which leads to the angular shift due to the difference in the sizes of In<sup>3+</sup> (0.81 Å) and Ni<sup>2+</sup> (0.69 Å) ions.

As NiO is introduced into the composites obtained by the hydrothermal method, the lattice parameters of both cubic and rhombohedral indium oxide decrease, which is also due to the difference in the ionic radii of In and Ni. In impregnated samples, the lattice parameters are – nickel is embedded in the structure of indium oxide in hydrothermal samples. In the case of impregnated samples, X-ray data indicate that amorphous NiO is formed on the surface of In<sub>2</sub>O<sub>3</sub>, but some Ni ions can be embedded in the near-surface layers.

The particle size calculated by the Debye–Scherrer formula is about 60 nm for impregnated composites and does not depend on the nickel oxide content. At the same time, in hydrothermal samples, the introduction of nickel into the indium oxide structure leads to a decrease in particle size from 34.5 to 30.5 nm for samples with a cubic structure and 24.6 to 15.5 nm for the rhombohedral phase. The introduction of nickel ions into different crystalline phases of In<sub>2</sub>O<sub>3</sub> hydrothermal composites prevents crystal growth. This finding is attributed to the occurrence of deformations due to indium substitution in the lattice.

TEM data for impregnated NiO–In<sub>2</sub>O<sub>3</sub> nanocomposites show that spherical particles of up to 20 nm in size are formed on the surface of indium oxide particles of about 100 nm size as a result of their impregnation with nickel nitrate and further heat treatment (Fig. 2(1)). Hydrothermal samples synthesized from an aqueous solution are agglomerates of

heterogeneous in size rectangular nanoparticles (Fig. 2(2)). The nanoparticles in the rhombohedral samples have a shape close to spherical and are uniform in size (Fig. 2(3)).

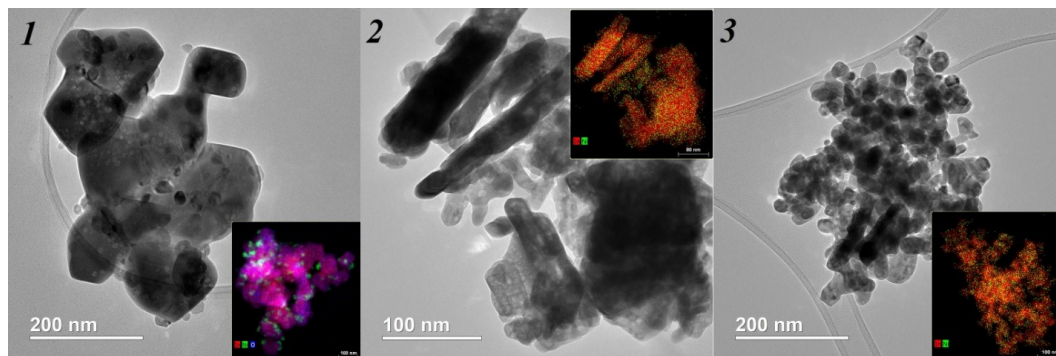


FIG. 2. TEM and EDA analysis (in the insert) of 3 % NiO – 97 % In<sub>2</sub>O<sub>3</sub> composites synthesized by impregnation (1) and hydrothermal method from solutions of indium and nickel nitrates in water (2) and ethanol (3)

The data on energy dispersion mapping of In, O and Ni in hydrothermal composites show that nickel ions are evenly distributed in indium oxide particles. The particles containing only nickel ions are also observed on the surface of indium oxide in impregnated composites. In the latter case, a small quantity of nickel is distributed in the surface layer of indium oxide particles.

The adsorption-desorption of nitrogen by the samples at 77 K was studied in order to determine the specific surface area and porosity of the synthesized samples. The isotherms of the impregnated samples have a shape characteristic of nonporous or macroporous samples (Fig. 3(1)). Regardless of the Ni content in such composites, the isotherms are almost identical, with only minor differences in the filling area of the macropores.

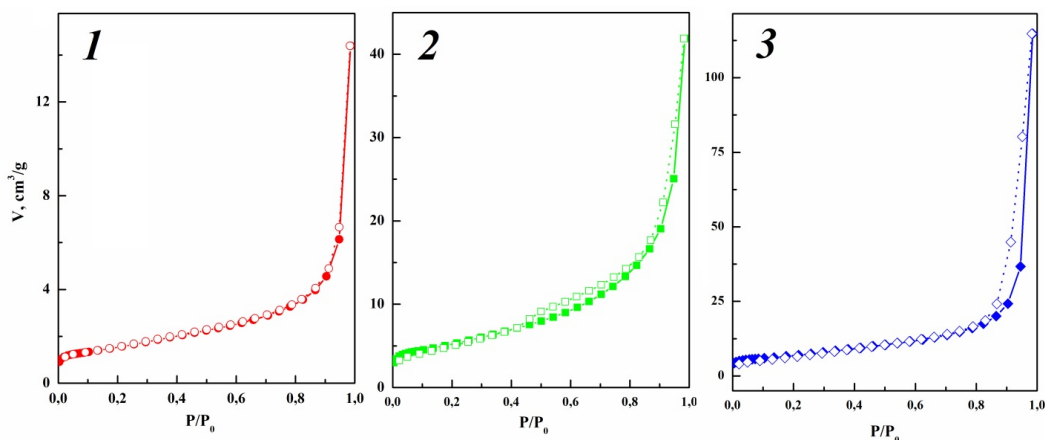


FIG. 3. Isotherms of adsorption (filled symbols) and desorption (empty symbols) of nitrogen at 77 K of 1 % NiO – 99 % In<sub>2</sub>O<sub>3</sub> composites synthesized by impregnation (1) and hydrothermal method using solutions of indium and nickel nitrates in water (2) and ethanol (3)

Based on the IUPAC classification, the isotherms of hydrothermal samples have a type IV shape with a hysteresis loop H3, which indicates a mesoporous nature of these samples (Fig. 3(2 and 3)). The shape of the hysteresis loop of hydrothermal composites depends on the mesoporous structure of the crystalline phase of indium oxide present in the samples. For composites with a rhombohedral structure (Fig. 3(3)) the hysteresis closes in the region of relative pressures  $P/P_0$  ( $P$  is the partial pressure of the adsorbed substance, and  $P_0$  is the pressure of saturated vapors of the adsorbed gas), close to 0.8. In addition, the hysteresis closes in the region of  $P/P_0$  values close to 0.4 in samples with a cubic structure of In<sub>2</sub>O<sub>3</sub> (Fig. 3(2)).

The specific surface area of impregnated composites ( $S_{\text{BET}}$ ), calculated by the BET method, is 5.1 – 5.6 m<sup>2</sup>/g and essentially independent of the concentration of NiO in the samples. For hydrothermal samples synthesized from an alcoholic solution, the  $S_{\text{BET}}$  value varies from 21.9 m<sup>2</sup>/g for pure In<sub>2</sub>O<sub>3</sub> to 26.1 m<sup>2</sup>/g for a sample containing 3 % NiO. Samples synthesized from an aqueous solution have a slightly lower specific surface area  $S_{\text{BET}}$ , which is 16.1 m<sup>2</sup>/g for pure In<sub>2</sub>O<sub>3</sub> and reaches 18.2 m<sup>2</sup>/g for a sample containing 3 % NiO. The specific surface area becomes greater with increase in the concentration of NiO in such composites.

The mesoporous structure of the samples, on which their sensor properties largely depend, was studied by the BJH method (Fig. 4). The pore size distribution for these samples also differs significantly. As can be seen from the data shown in Fig. 4, the diameter of the mesopores of the rhombohedral hydrothermal sample synthesized from an alcoholic solution is mainly 20 nm. In the diagram of this sample there is also a very small peak in the 3 nm region, but the total pore volume of this size is negligible compared to the pore volume of a larger diameter. With an increase in the concentration of NiO in such composites, the volume of mesopores increases, which leads to an increase in the specific surface area  $S_{\text{BET}}$ .

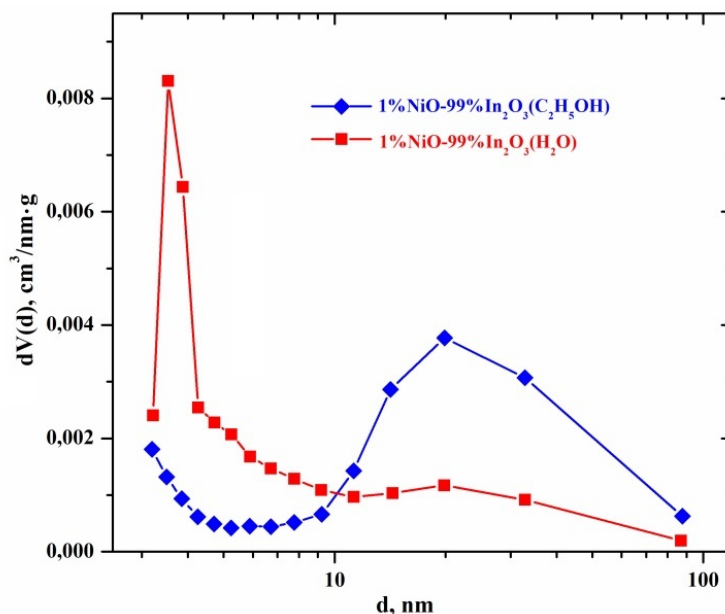


FIG. 4. Pore size distribution for hydrothermal samples containing 1 % NiO

The pore size distribution for hydrothermal samples of cubic structure has an acute peak in the region of pores with a diameter of 3.5 nm, followed by a wide decreasing plume of pores with a larger diameter (see Fig. 4). With an increase in the concentration of NiO in composites of this type, the volume of mesopores increases slightly. This, apparently, explains the smaller increase in the specific surface area  $S_{\text{BET}}$  of such samples compared to nanocomposites of rhombohedral structure. In addition, the total volume of 3.5 nm pores in samples synthesized from aqueous solution is approximately 3 times smaller than the total volume of 20 nm pores for samples synthesized from ethanol. It can be assumed that in hydrothermal composites of cubic structure, narrow pores with a diameter of 3.5 nm correspond to pores inside the nanoparticles, while in samples with a rhombohedral structure, 20 nm pores correspond to pores between the nanoparticles.

The composition and valence state of the surface elements and active oxygen centers were determined by the XPS method. Only peaks In, O, C and Ni are present in the survey spectra, which indicates the high purity of the synthesized samples. Two intense peaks with binding energies of 452.3 and 444.7 eV, observed for all samples, belong to the spin-orbital energy states In 3d<sub>3/2</sub> and In 3d<sub>5/2</sub>, respectively (Fig. 5). The XPS study indicates that the valence state of indium ions in the samples is 3+.

It should be noted that regardless of the method of obtaining NiO–In<sub>2</sub>O<sub>3</sub>, the introduction of NiO in the composite leads to a decrease in the binding energy In 3d<sub>3/2</sub> and In 3d<sub>5/2</sub>. This result is due to the substitution of nickel ions in the crystal lattice, leading to the formation of In–O–Ni with a relatively low binding energy, and once again indicates the introduction of Ni into the In<sub>2</sub>O<sub>3</sub> lattice. In the high-resolution Ni 2p XPS spectra for all the composites obtained, peaks characterized by binding energies of 854 and 873 eV are observed, which corresponds to the valence state 2+ of nickel ions. The spectra of XPS O 1s are also analyzed in this study. The asymmetric peak of O 1s can be divided into several peaks that are characteristic of three forms of oxygen, namely: lattice oxygen ( $O_L$ ) with a binding energy of 530.1 eV, oxygen vacancies ( $O_V$ ) with a binding energy of 531.5 eV and chemisorbed oxygen ( $O_C$ ) with a binding energy of 532.4 eV (see Fig. 6).

The  $O_L$  signal is caused by the presence of  $O^{2-}$  ions in the crystal structure. The  $O_V$  characterizes the region of oxygen vacancies in the matrix and plays an important role in gas-sensitive characteristics. The  $O_C$  is associated with oxygen ions adsorbed on the surface of the sample. The content of various oxygen forms in the samples depends on the synthesis method. Thus, the impregnation of In<sub>2</sub>O<sub>3</sub> with nickel nitrate leads to a decrease in the number of oxygen vacancies by 8 % and an increase in the concentration of chemisorbed oxygen by 17 %. In hydrothermal samples, the introduction of NiO increases the number of oxygen vacancies by 18 % for the cubic In<sub>2</sub>O<sub>3</sub> phase and 2 % for

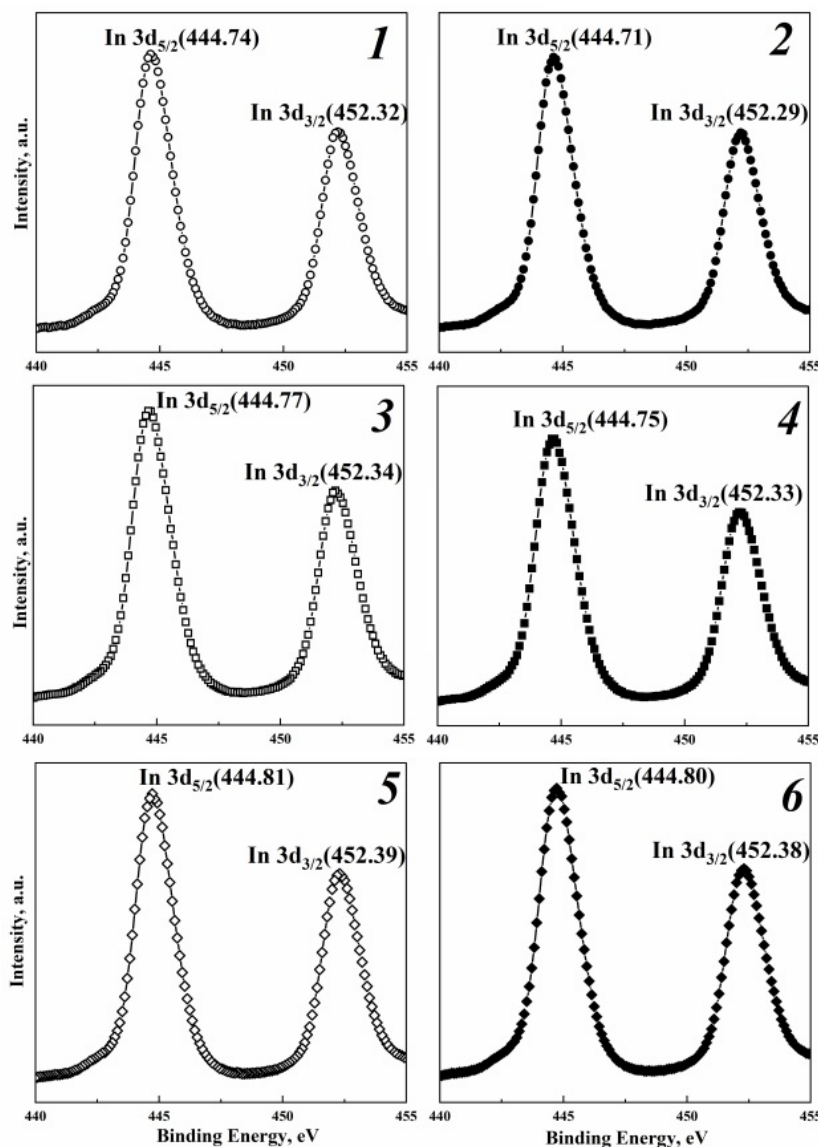


FIG. 5. High-resolution XPS spectra In 3d:  $\text{In}_2\text{O}_3$  (1), impregnated composite of 1 % NiO – 99 %  $\text{In}_2\text{O}_3$  (2), hydrothermal samples  $\text{In}_2\text{O}_3$  (3) and 3 % NiO – 97 %  $\text{In}_2\text{O}_3$  (4) synthesized from aqueous solutions of In and Ni salts, as well as  $\text{In}_2\text{O}_3$  (5) and 3 % NiO – 97 %  $\text{In}_2\text{O}_3$  (6) synthesized from salt solutions in ethanol

the rhombohedral phase and thereby affects the sensory activity of the composites. In addition, the concentration of chemisorbed oxygen decreases in the composites with a cubic structure but increases in rhombohedral samples.

### 3.2. Conductivity of NiO– $\text{In}_2\text{O}_3$ composites

The conductivity of NiO– $\text{In}_2\text{O}_3$  composites synthesized by different methods are enhanced with the increase of sensor layer temperature from 300 to 520 °C (Fig. 7), which is typical for n-type semiconductors. Moreover, violations of this pattern decrease with increase in the fraction of nickel oxide. This trend is not surprising considering the peculiarities of the temperature dependence of  $\text{In}_2\text{O}_3$  conductivity [21]. The composites synthesized by  $\text{In}_2\text{O}_3$  impregnation with nickel nitrate have the highest conductivity at all the temperatures investigated.

It was also found that the conductivity of the composites decreases with an increase in the nickel oxide content (see Fig. 7(4)). In the process of impregnation, X-ray amorphous NiO is formed on the surface of indium oxide nanoparticles, while some nickel ions can be embedded in its near-surface layers. The electron work function from NiO (5.5 eV) is higher than from indium oxide (4.3 eV). Thus, upon contact of these oxides, electrons are transferred from  $\text{In}_2\text{O}_3$  nanoparticles with a high concentration of conduction electrons to the NiO nanoparticles. This transfer is accompanied by a decrease in the conductivity of the composites.

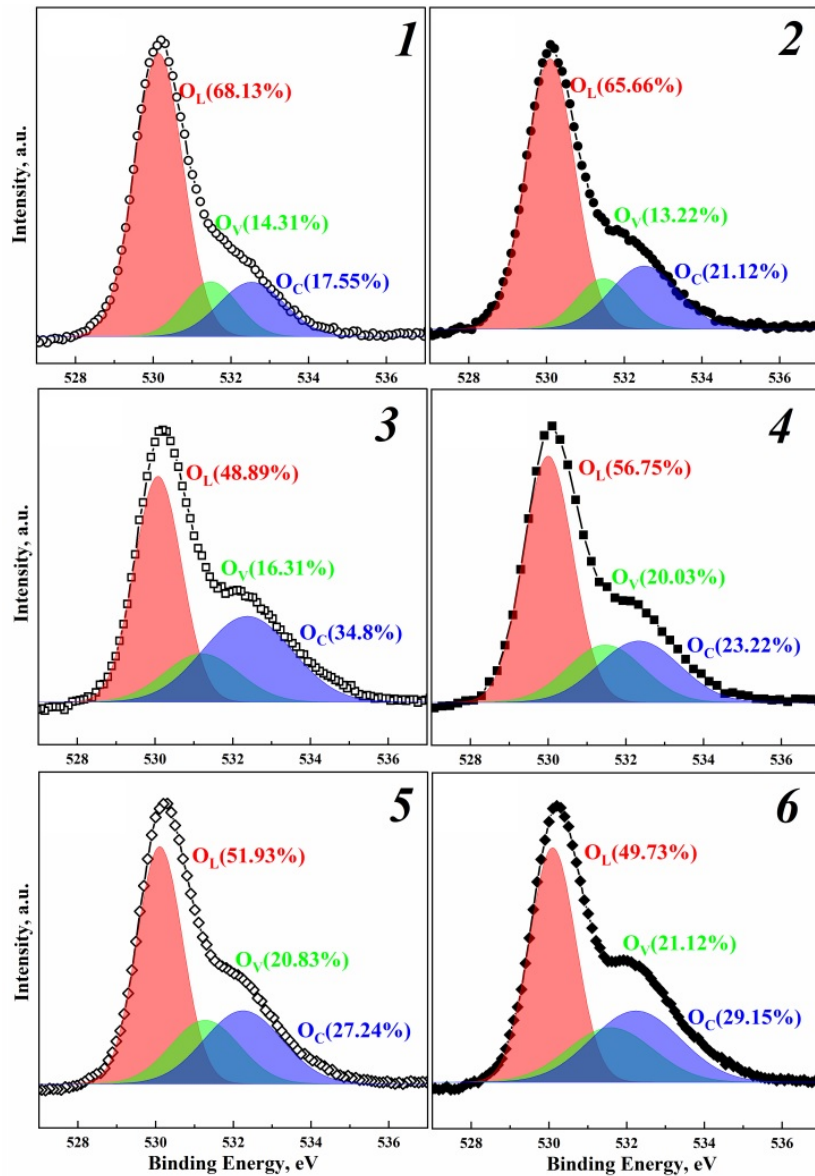


FIG. 6. High-resolution XPS spectra of O 1s: (1) In<sub>2</sub>O<sub>3</sub>; (2) composite 1 % NiO – 99 % In<sub>2</sub>O<sub>3</sub> obtained by impregnation; hydrothermal samples synthesized from aqueous solutions of indium and nickel nitrates: In<sub>2</sub>O<sub>3</sub> (3) and 3 % NiO – 97 % In<sub>2</sub>O<sub>3</sub> (4); hydrothermal samples synthesized from solutions of salts in ethanol: In<sub>2</sub>O<sub>3</sub> (5) and 3 % NiO – 97 % In<sub>2</sub>O<sub>3</sub> (6)

In the process of hydrothermal synthesis, nickel ions (Ni<sup>2+</sup>) are introduced into the lattice of both cubic and rhombohedral In<sub>2</sub>O<sub>3</sub>, replacing In<sup>3+</sup> ions. In addition, positively charged oxygen vacancies V<sub>O</sub><sup>+</sup> are formed in the composite, which ensures a balance of positive and negative charges.

The conductivity of hydrothermal composites, regardless of the nature of the In<sub>2</sub>O<sub>3</sub> crystalline phase, is an order of magnitude lower than that of impregnated ones. This result is due to the fact that during the hydrothermal synthesis of composites, the quantity of In<sup>3+</sup> ions replaced by Ni<sup>2+</sup> ions is greater than during impregnation. This in turn leads to a decrease in the conductivity of hydrothermal samples relative to impregnated ones. It should also be noted that the interaction of nanoparticles during impregnation is concentrated mainly in the surface layers of the nanocrystals. In addition, the conductivity of hydrothermal composites depends on the phase state of the In<sub>2</sub>O<sub>3</sub> crystals.

Composites with a rhombohedral structure have higher conductivity than similar composites of a cubic structure (see Fig. 7(4)). In the rhombohedral lattice of In<sub>2</sub>O<sub>3</sub> crystals, unlike the cubic type, there are elongated and, consequently, weakened In–O bonds. This may be responsible for the increase in the concentration of vacancies and the corresponding increase in the concentration of conduction electrons generated by these vacancies in the composites with a rhombohedral structure compared to a cubic structure.

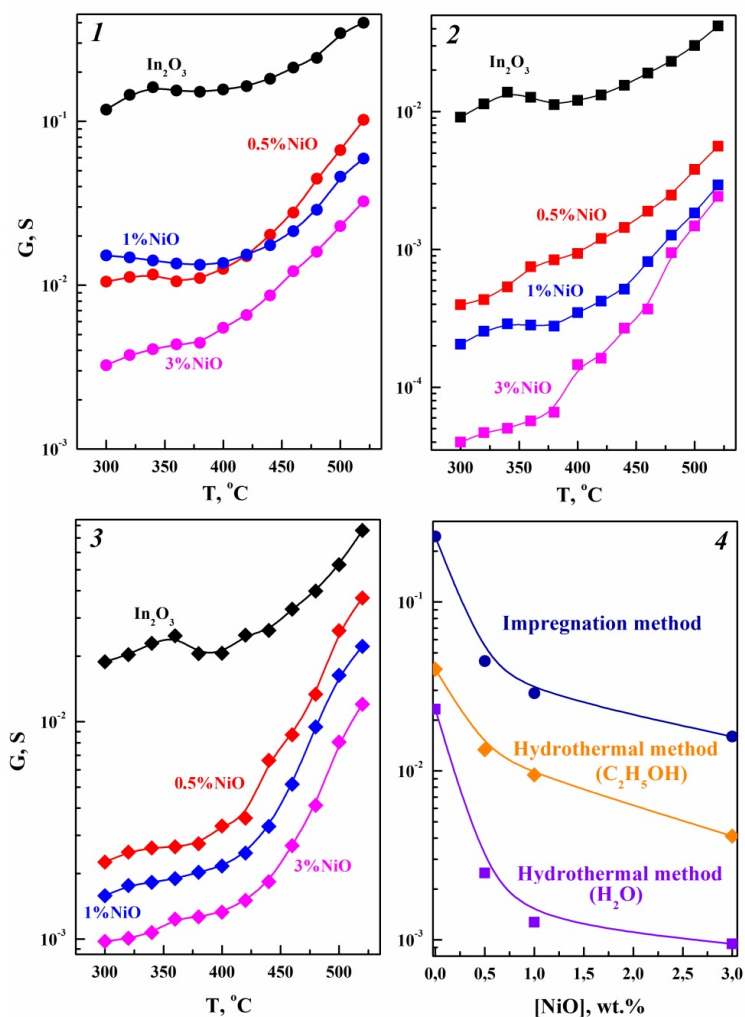


FIG. 7. Temperature dependence of the conductivity of NiO–In<sub>2</sub>O<sub>3</sub> composites synthesized by impregnation (1) and hydrothermal method using solutions of indium and nickel nitrates in water (2) and ethanol (3). Dependence of the conductivity of NiO–In<sub>2</sub>O<sub>3</sub> composites synthesized by different methods on the concentration of NiO at  $T = 460$  °C (4)

### 3.3. Sensor properties of NiO–In<sub>2</sub>O<sub>3</sub> composites

In NiO–In<sub>2</sub>O<sub>3</sub> composites, regardless of the synthesis method, the temperature dependence of sensor response to H<sub>2</sub> and CO has a curve that is typical for semiconductor sensors with a maximum  $S_{\max}$  at a certain temperature  $T_{\max}$  (see Fig. 8). In all cases, the sensor activity of composites exceeds the activity of pure In<sub>2</sub>O<sub>3</sub> (Fig. 9).

Oxygen vacancies are centers of chemisorption of oxygen and the analyzed gas, therefore, an increase in their concentration contributes to a higher sensor response of rhombohedral indium oxide. Since the introduction of nickel oxide in the sample enhances the number of vacancies, the sensor response increases accordingly. In addition, the magnitude of the response to different concentrations of hydrogen and carbon monoxide depends on the method used for synthesizing the composite (see Fig. 9).

A hydrothermal composite of 3 % NiO – 97 % In<sub>2</sub>O<sub>3</sub> synthesized from an alcoholic solution of the corresponding nitrates and containing rhombohedral indium oxide has the highest sensor response to 0.9 % H<sub>2</sub>. However, at 0.1 % H<sub>2</sub> detection, the highest response has the hydrothermal composite 3 % NiO – 97 % In<sub>2</sub>O<sub>3</sub>, synthesized from an aqueous solution in which cubic indium oxide is present. When detecting carbon monoxide, the hydrothermal composite based on cubic indium oxide containing 3 % nickel oxide shows the highest efficiency. It should be noted that impregnated composites have the lowest response to hydrogen and carbon monoxide, which is due to the lower specific surface area of such samples compared to hydrothermal samples.

The method of synthesis of NiO–In<sub>2</sub>O<sub>3</sub> composites significantly affects the dependence of the sensor response on the concentration of nickel oxide (Fig. 9). The highest efficiency of impregnated samples is observed when they contain 0.5 – 1 % NiO.

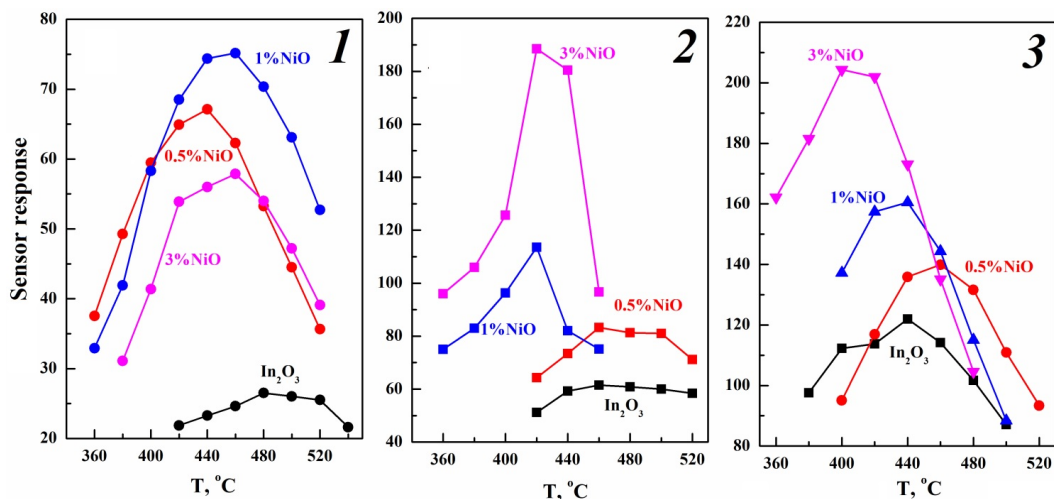


FIG. 8. Temperature dependences of the sensor response to 0.9 % H<sub>2</sub> of NiO–In<sub>2</sub>O<sub>3</sub> composites synthesized by impregnation (1) and hydrothermal method using solutions of indium and nickel nitrates in water (2) and ethanol (3)

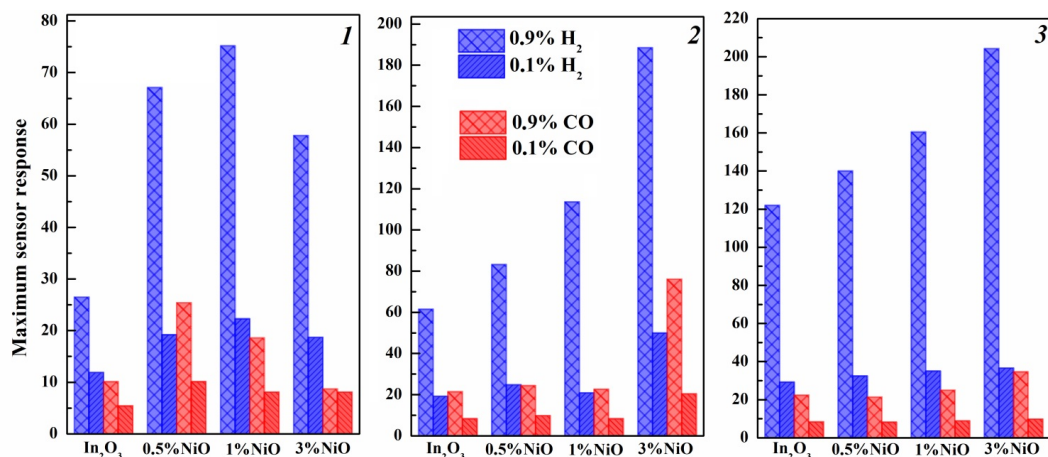


FIG. 9. Concentration dependence of the maximum sensor response to different concentrations of H<sub>2</sub> and CO of NiO–In<sub>2</sub>O<sub>3</sub> composites synthesized by impregnation (1) and hydrothermal method using solutions of indium and nickel nitrates in water (2) and ethanol (3)

A further increase of the NiO content in impregnated composites results in a slight decrease in sensor response, while the addition of 3 % NiO to a hydrothermal composite causes a sharp increase in the sensitivity to H<sub>2</sub> and CO. Such a behavior takes place due to the various types of interactions between the components in the composites synthesized by different methods.

Nickel ions are embedded in the indium oxide lattice in hydrothermal samples, which leads to an increase in the defectiveness of the nanoparticles, the concentration of atomic oxygen on the surface and the sensor effect. In composites synthesized by impregnation, NiO nanoclusters are formed on the surface of In<sub>2</sub>O<sub>3</sub> nanoparticles and do not affect their structure, size and defects. Consequently, nickel oxide additives in this case have a lesser effect on the sensor response compared to hydrothermal samples. It should be noted that the mechanisms considered here affecting the response of sensors prepared by impregnation and hydrothermal method differ from the mechanism proposed in [20], where samples were obtained by electrospinning and calcination methods. The increased sensitivity with the addition of nickel oxide was attributed to the formation of p-n-transitions between NiO and In<sub>2</sub>O<sub>3</sub> and a decrease in particle size.

An increase in the nickel oxide content leads to a decrease in the optimal operating temperature for hydrothermal samples by 40 – 60 °C, and for impregnated samples by 20 °C. This decrease is caused by the high catalytic activity of NiO nanoparticles.

A comparison of the sensor properties of indium oxide and NiO–In<sub>2</sub>O<sub>3</sub> composites obtained by different methods and under various conditions is presented in Table 1.

TABLE 1. Sensor properties of NiO and In<sub>2</sub>O<sub>3</sub>-based materials at detecting different concentrations of H<sub>2</sub> and CO

Sample	Synthesis method	Gas concentration	Sensor response	T, °C	Reference
In <sub>2</sub> O <sub>3</sub>	one-step hydrothermal and thermal treatment process using MOF	100 ppm H <sub>2</sub>	7.9	100	[22]
3 % Ni–In <sub>2</sub> O <sub>3</sub>			12.5		
In <sub>2</sub> O <sub>3</sub>	solvothermal method	10 ppm CO	2.5	200	[23]
1 % Ni–In <sub>2</sub> O <sub>3</sub>			4.8		
In <sub>2</sub> O <sub>3</sub>	nanocasting method	1 ppm CO	—	58	[24]
Ni-doped In <sub>2</sub> O <sub>3</sub>			2.7		
In <sub>2</sub> O <sub>3</sub>	solvothermal method	100 ppm CO	2	140	[25]
5 % Ni–In <sub>2</sub> O <sub>3</sub>			11.03		
In <sub>2</sub> O <sub>3</sub>	hydrothermal method	100 ppm H <sub>2</sub>	4.8	150	[26]
NiO/In <sub>2</sub> O <sub>3</sub> – 0.2		100 ppm CO	1.2		
		100 ppm H <sub>2</sub>	4.9		
		100 ppm CO	1.3		
In <sub>2</sub> O <sub>3</sub>	hydrothermal method	100 ppm CO	1.2	280	[27]
NiIn – 2			6.4		
In <sub>2</sub> O <sub>3</sub>	impregnation method	0.9 % / 0.1 % H <sub>2</sub>	26.5/11.9	480	<b>This work</b>
1 % NiO–In <sub>2</sub> O <sub>3</sub>		0.9 % / 0.1 % CO	10.1/5.4		
		0.9 % / 0.1 % H <sub>2</sub>	75.2/22.3	460	
		0.9 % / 0.1 % CO	18.6/8.1		
In <sub>2</sub> O <sub>3</sub>	hydrothermal method (water)	0.9 % / 0.1 % H <sub>2</sub>	61.5/19.2	460	<b>This work</b>
3 % NiO–In <sub>2</sub> O <sub>3</sub>		0.9 % / 0.1 % CO	21.4/8.3		
		0.9 % / 0.1 % H <sub>2</sub>	188.5/49.9	400	
		0.9 % / 0.1 % CO	76.1/20.4		
In <sub>2</sub> O <sub>3</sub>	hydrothermal method (ethanol)	0.9 % / 0.1 % H <sub>2</sub>	122/29.2	440	<b>This work</b>
3 % NiO–In <sub>2</sub> O <sub>3</sub>		0.9 % / 0.1 % CO	22.36/8.4		
		0.9 % / 0.1 % H <sub>2</sub>	204.3/36.6	400	
		0.9 % / 0.1 % CO	34.6/8.9		

It turned out that the introduction of nickel into indium oxide at various concentrations of the additive, regardless of the production method, increases the sensor response. Compared with the literature data, the NiO–In<sub>2</sub>O<sub>3</sub> composites synthesized by us have higher sensory response values to H<sub>2</sub> and CO, but at a higher operating temperature. The introduction of nickel results in a decrease of operating temperature compared to pure indium oxide, which was not observed in other studies. Note also that in works [22–27], the composites based on NiO–In<sub>2</sub>O<sub>3</sub> containing only the cubic phase of indium oxide are considered. We have shown that the magnitude of the sensor response and selectivity in detecting H<sub>2</sub> and CO are higher for composites based on rhombohedral In<sub>2</sub>O<sub>3</sub> than for cubic ones.

The response/recovery time of samples when detecting 0.9 % hydrogen depends on the method of sample preparation. However, in all cases, the introduction of nickel oxide into the composite leads to a decrease in the response and recovery time of the sensor. Thus, with the introduction of 1 % NiO in impregnated samples, the response time decreases from 1.3 to 0.8 s, and the recovery time – from 6.5 to 5.4 s. In the case of samples obtained by the hydrothermal method and having cubic structure,  $t_{\text{resp}}$  decreases from 0.4 to 0.2 s, and  $t_{\text{rec}}$  from 14 to 10 s, and in the samples with a rhombohedral structure,  $t_{\text{resp}}$  decreases from 0.3 to 0.1 s,  $t_{\text{rec}}$  from 5 to 4.7 s. A longer recovery time compared to other samples is also observed in hydrothermal sensitive layers with a cubic structure of indium oxide.

The sensor properties of the synthesized samples were measured regularly for 5 months at the optimal operating temperature. Over this period, the resistance of the sensor layer in the air and the magnitude of the response to H<sub>2</sub> were found to vary by less than 5 – 10 % depending on the synthesis method, indicating the long-term stability of the samples obtained.

#### 4. Conclusions

Composites consisting of metal oxides with different types of conductivity (In<sub>2</sub>O<sub>3</sub> and NiO) have been synthesized by impregnation and hydrothermal methods. The structural characteristics, as well as conductive and sensor properties of the samples obtained have been studied. It is shown that the introduction of NiO into composites obtained by the hydrothermal method leads to a decrease in the value of In<sub>2</sub>O<sub>3</sub> lattice parameters. The lattice parameters in impregnated samples are practically independent of the NiO content.

The specific surface area of impregnated composites is 5.1 – 5.6 m<sup>2</sup>/g and does not depend much on the concentration of NiO in the samples. However, the addition of 3 % NiO to indium oxide increases the specific surface area of a hydrothermal sample with rhombohedral structure from 21.9 to 26.1 m<sup>2</sup>/g and from 16.1 to 18.2 m<sup>2</sup>/g for samples with cubic structure. The conductivity of hydrothermal composites is an order of magnitude lower than that of impregnated composites. It is shown that an increase in the NiO content in the composite leads to an increase in their sensor response to H<sub>2</sub> and CO, as well as a decrease in the optimal operating temperature for hydrothermal samples by 60 °C, and for impregnated samples by 20 °C.

The conducted studies allowed us to compare the properties of NiO–In<sub>2</sub>O<sub>3</sub> sensor systems depending on the synthesis method used. Thus, the maximum response to 0.9 % H<sub>2</sub> sensors, with a sensitive layer prepared by the impregnation method, was achieved when the NiO additive was 1 %, but the optimal additive value at the hydrothermal method was 3 %. At the same time, the maximum response value was slightly larger for sensors prepared using solutions of indium and nickel nitrates in ethanol. Note that in this case, rhombohedral indium oxide is formed. However, the maximum response to 0.1 % H<sub>2</sub> is achieved for the sensitive layer obtained using solutions nitrates in water with cubic indium oxide. In other words, the properties of the studied systems are strongly dependent not only on the method of preparation and concentration of the additive, but also on the concentration of the gas being studied. It is also important that the introduction of nickel oxide into the composite leads to a decrease in the optimal operating temperature and response/recovery time of the sensor, as well as to an increase in selectivity.

It follows from the above that sensors prepared by hydrothermal method are more effective compared to impregnated systems. The choice between using alcohol or water as a solvent for hydrothermal synthesis of the sensitive layer depends on which sensor characteristic is most important in a particular case.

#### References

- [1] Zappa D., Galstyan V., Kaur N., Arachchige H.M.M., Sisman O., Comini E. Metal oxide-based heterostructures for gas sensors – A review. *Anal. Chim. Acta*, 2018, **1039**, P. 1–23.
- [2] Gerasimov G.N., Gromov V.F., Ilegbusi O.J., Trakhtenberg L.I. The mechanisms of sensory phenomena in binary metal-oxide nanocomposites. *Sens. Actuators B Chem.*, 2017, **240**, P. 613–624.
- [3] Hu J., Sun Y., Xue Y., Zhang M., Li P., Lian K., Chen Y. Highly sensitive and ultra-fast gas sensor based on CeO<sub>2</sub>-loaded In<sub>2</sub>O<sub>3</sub> hollow spheres for ppb-level hydrogen detection. *Sens. Actuators B Chem.*, 2018, **257**, P. 124–135.
- [4] Vasiliev A., Shaposhnik A., Moskalev P., Kul O. Kinetics of chemisorption on the surface of nanodispersed SnO<sub>2</sub>-PdO<sub>x</sub> and selective determination of CO and H<sub>2</sub> in air. *Sensor*, 2023, **23**, 3730.
- [5] Kim H.J., Lee J.H. Highly sensitive and selective gas sensors using p-type oxide semiconductors: overview. *Sens. Actuators B Chem.*, 2014, **192**, P. 607–627.
- [6] Xu K., Duan S.L., Tang Q., Zhu Q., Zhao W., Yu X., Yang Y., Yu T., Yuan C.L., P-N heterointerface-determined acetone sensing characteristics in α-MoO<sub>3</sub>-NiO core-shell nanobelts. *Cryst. Eng. Comm.*, 2019, **21**, P. 5834–5844.
- [7] Kavitha G., Arul K.T., Babu P. Enhanced acetone gas sensing behavior of n-ZnO/p-NiO nanostructures. *J. Mater. Sci.: Mater. Electron.*, 2018, **29**, P. 6666–6671.
- [8] Choi S., Lee J.K., Lee W.S., Lee C., Lee W.I. Acetone sensing of multi-networked WO<sub>3</sub>-NiO core-shell nanorod sensors. *J. Korean Phys. Soc.*, 2017, **71**, P. 487–493.
- [9] Sun G.J., Kheel H., Choi S., Hyun S.K., Lee C. Prominent gas sensing performance of TiO<sub>2</sub>-core/NiO-shell nanorod sensors. *J. Nanosci. Nanotechnol.*, 2017, **17**, P. 4099–4102.
- [10] Haq M.U., Wen Z., Zhang Z.Y., Khan S., Lou Z.R., Ye Z.Z., Zhu L.P. A two-step synthesis of nanosheet-covered fibers based on α-Fe<sub>2</sub>O<sub>3</sub>/NiO composites towards enhanced acetone sensing. *Sci. Rep.*, 2018, **8**, 1705.
- [11] Lee H., Mirzaei A., Kim H.W., Kim S.S. SnO<sub>2</sub>(n)-NiO(p) composite nanowires: Gas sensing properties and sensing mechanisms. *Sens. Actuators B Chem.*, 2018, **258**, P. 204–214.
- [12] Ikim M.I., Gerasimov G.N., Gromov V.F., Ilegbusi O.J., Trakhtenberg L.I. Synthesis, structural and sensor properties of nanosized mixed oxides based on In<sub>2</sub>O<sub>3</sub> particles. *Int. J. Mol. Sci.*, 2023, **24**, 1570.
- [13] Katoch A., Choi S.-W., Kim J.-H., Lee J.-H., Lee J.-S., Kim S.S. Importance of the nanograin size on the H<sub>2</sub>S-sensing properties of ZnO-CuO composite nanofibers. *Sens. Actuators B Chem.*, 2015, **214**, P. 111–116.
- [14] Choi S.-W., Zhang J., Katoch A., Kim S.S. H<sub>2</sub>S sensing performance of electrospun CuO-loaded SnO<sub>2</sub> nanofibers. *Sens. Actuators B Chem.*, 2012, **160**, P. 54–60.
- [15] Liu Y., Bai J., Li Y., Yang L., Wang Y., Li Y., Liu F., Zhang Y., Lu G. Preparation of PdO-decorated NiO porous film on ceramic substrate for highly selective and sensitive H<sub>2</sub>S detection. *Ceramics Int.*, 2022, **48**, P. 4787–4794.
- [16] Liu H., Wang Z., Cao G., Pan G., Yang X., Qiu M., Sun C., Shao J., Li Z., Zhang H. Construction of hollow NiO/ZnO p-n heterostructure for ultrahigh performance toluene gas sensor. *Mater. Sci. in Semicond. Proc.*, 2022, **141**, 106435.
- [17] Ju D., Xu H., Xu Q., Gong H., Qiu Z., Guo J., Zhang J., Cao B. High triethylamine-sensing properties of NiO/SnO<sub>2</sub> hollow sphere P-N hetero-junction sensors. *Sens. Actuators B Chem.*, 2015, **215**, P. 39–44.
- [18] Kaur M., Dadhich B.K., Singh R., Ganapathi K., Bagwaiya T., Bhattacharya S., Gadkari S.C., RF sputtered SnO<sub>2</sub>: NiO thin films as sub-ppm H<sub>2</sub>S sensor operable at room temperature. *Sens. Actuators B Chem.*, 2017, **242**, P. 389–403.

- [19] Fan X., Xu Y., He W. High acetone sensing properties of In<sub>2</sub>O<sub>3</sub>-NiO one-dimensional heterogeneous nanofibers based on electrospinning. *RSC Advances.*, 2021, **19**, P. 11215–11223.
- [20] Yan C., Lu H.B., Gao J.Z., Zhu G.Q., Yin F., Yang Z.B., Liu Q.R., Li G. Synthesis of porous NiO-In<sub>2</sub>O<sub>3</sub> composite nanofibers by electrospinning and their highly enhanced gas sensing properties. *J. Alloys Compd.*, 2017, **699**, P. 567–574.
- [21] Belysheva T.V., Gerasimov G.N., Gromov V.F., Spiridonova E.Yu., Trakhtenberg L.I. Conductivity of SnO<sub>2</sub>-In<sub>2</sub>O<sub>3</sub> nanocrystalline composite films. *Russ. J. Phys. Chem. A*, 2010, **84**, P. 1554–1559.
- [22] Qin W., Lu B., Xu X., Shen Y., Meng F. Metal organic framework-derived porous Ni-doped In<sub>2</sub>O<sub>3</sub> for highly sensitive and selective detection to hydrogen at low temperature. *Sens. Actuators B Chem.*, 2024, **417**, 136123.
- [23] Jin Z., Wang C., Wu L., Song H., Yao X., Liu J., Wang, F. Fast responding and recovering of NO<sub>2</sub> sensors based on Ni-doped In<sub>2</sub>O<sub>3</sub> nanoparticles. *Sens. Actuators B Chem.*, 2023, **377**, 133058.
- [24] Yang Q., Cui X., Liu J., Zhao J., Wang Y., Gao, Y., Lu G. A low temperature operating gas sensor with high response to NO<sub>2</sub> based on ordered mesoporous Ni-doped In<sub>2</sub>O<sub>3</sub>. *New J. Chem.*, 2016, **40** (3), P. 2376–2382.
- [25] Zhang Y., Cao J., Wang Y. Ultrahigh methane sensing properties based on Ni-doped hierarchical porous In<sub>2</sub>O<sub>3</sub> microspheres at low temperature. *Vacuum*, 2022, **202**, 111149.
- [26] Liang Z., Zhang Y., Wang M., Liu S., Zhang X., Lei S., Liu G. Facile preparation of flower-like NiO/In<sub>2</sub>O<sub>3</sub> composite for sensitively and selectively detecting NO<sub>2</sub> at room and lower temperatures. *Appl. Surf. Sci.*, 2024, **657**, 159805.
- [27] Zhang S., Li J., Han L., Zhang B., Wang Y., Zhang Z. Preparation of porous NiO/In<sub>2</sub>O<sub>3</sub> nanoflower-like composites and their dual selectivity for CO/CH<sub>4</sub>. *Mater. Res. Bull.*, 2023, **165**, 112332.

---

Submitted 1 July 2024; revised 29 August 2024; accepted 13 October 2024

*Information about the authors:*

*Mariya I. Ikim* – N. N. Semenov Federal Research Center for Chemical Physics RAS, 4 Kosygin Street, Moscow, 119991, Russia; ORCID 0000-0003-4411-1119; ikimmary1104@gmail.com

*Vladimir F. Gromov* – N. N. Semenov Federal Research Center for Chemical Physics RAS, 4 Kosygin Street, Moscow, 119991, Russia; ORCID 0000-0002-9401-1717; vfgromov@mail.ru

*Genrikh N. Gerasimov* – N. N. Semenov Federal Research Center for Chemical Physics RAS, 4 Kosygin Street, Moscow, 119991, Russia; ORCID 0000-0001-8692-0382; gerasimovgen@mail.ru

*Valentin G. Bekeshev* – N. N. Semenov Federal Research Center for Chemical Physics RAS, 4 Kosygin Street, Moscow, 119991, Russia; ORCID 0000-0001-8989-3965; bvg495@yandex.ru

*Leonid I. Trakhtenberg* – N. N. Semenov Federal Research Center for Chemical Physics RAS, 4 Kosygin Street, Moscow, 119991, Russia; Chemical Faculty, Lomonosov Moscow State University, Moscow, 119991, Russia; Moscow Institute of Physics and Technology(State University), Moscow, Russia; ORCID 0000-0001-9139-5754; litrakh@gmail.com

*Conflict of interest:* the authors declare no conflict of interest.